Build Simul (2024) 17: 235–252
https://doi.org/10.1007/s12273-023-1082-5

Economic analysis of rooftop photovoltaics system under different shadowing conditions for 20 cities in China

Zhiyi Ren[1], Yixing Chen[1,2] (✉), Chengcheng Song[1], Mengyue Liu[1], Anni Xu[1], Qilin Zhang[1]

1. College of Civil Engineering, Hunan University, Changsha 410082, China
2. Key Laboratory of Building Safety and Energy Efficiency of Ministry of Education, Hunan University, Changsha 410082, China

Abstract

Installing photovoltaic (PV) systems is an essential step for low-carbon development. The economics of PV systems are strongly impacted by the electricity price and the shadowing effect from neighboring buildings. This study evaluates the PV generation potential and economics of 20 cities in China under three shadowing conditions. First, the building geometry models under three shadowing conditions for the 20 cities were constructed using QGIS. Then, 60 building models with PV systems and shadows from surrounding buildings were generated by City Buildings, Energy, and Sustainability (CityBES), an open platform, to simulate the PV power generation. Finally, the study presented one economic analysis model to evaluate the profitability by combining the market cost of rooftop PV systems and electricity prices in China. The economic model included four indicators: payback period (static and dynamic), net present value (NPV), and internal rate of return (IRR). The results show that the reduction of PV power generation ranges from 8.29% to 16.01% under medium shadowing, and experiences a maximum decrease of up to 39.71% under high shadowing. Further economic analysis shows that almost all the regions show reliable potential, obtaining an IRR higher than the reference value (5%). Nenjiang has the highest economic profit, with the highest NPV (86,181.15 RMB) and IRR (30.14%) under no shadowing among 20 cities. It also should be mentioned that the alignment between electricity price distribution and the solar power generation curve will directly impact the economic potential of PV systems.

Keywords

rooftop photovoltaic system
EnergyPlus
economic analysis
shadowing buildings
electric price

Article History

Received: 16 July 2023
Revised: 11 September 2023
Accepted: 29 September 2023

1 Introduction

China's photovoltaic (PV) market, an emerging industry with vast territory and abundant solar resources, is rapidly developing (Zhao et al. 2015). In 2022, China's new PV installed capacity was 87.41 GW, including 36.3 GW centralized PV power station and 51.11 GW distributed PV. The newly installed capacity of household distributed PV was 25.25 GW, up 17.3% year on year (CPIA 2022).

Rooftop PV power stations are preferred by investors due to their proximity to relatively low installation costs compared to large power stations (Thiem et al. 2017; Viana et al. 2018). Much research has investigated the development of small-scale PV systems (Yuan et al. 2014; Martinopoulos 2020), mainly involving regional development potential, subsidy price policy, production cost, and economic performance. Li et al. (2018) evaluated and concluded that grid/PV systems are technically, economically, and environmentally feasible for five climate zones in China. The excess electricity, NPC, and COE values of the grid/PV systems for all five climate zones increased with PV penetration increased. Considering incentive policies, Spertino et al. (2013) provided a technical-economic analysis of investments in PV systems installed on the rooftop. They applied it to some significant case studies in the countries where the PV market is the most prosperous (Germany and Italy). The analysis shows that incentive policies bring noticeable installation volume increments and cost decrements in the two PV markets. Lazzeroni et al. (2020) explored the feasibility of PV installation in different configurations considering

E-mail: yixingchen@hnu.edu.cn

the increasing electricity consumption of residential end-users. The results highlight how the perspective of PV investment remains positive even if a feed-in tariff for PV production is no longer available. Bergamasco and Asinari (2011) found that among the rooftop PV utilization potentials in the larger area of Italy, the roofing installation factors were classified based on the type of building, and the roofing installation factors for residential and industrial buildings were 0.7 and 0.9, respectively.

In the early stages of a developing industry, subsidy policies are often implemented as a form of financial aid to support the growth and advancement of the industry (Bazilian et al. 2013; Reichelstein and Yorston 2013). But, since 2022, the policy subsidies for distributed PV projects in China have almost been eliminated. The power of rooftop PV systems can directly meet the power demand of buildings, called PV self-consumption (Lang et al. 2016). Self-consumption has begun to evolve into a core driver of the economic performance of rooftop PV, providing a promising alternative to the subsidized feed-in tariff (Staudacher and Eller 2012; Lang et al. 2015). Graebig et al. (2014) found that self-consumption, as a goal in and of itself, is as essential for consumers as economic considerations in determining their interest in PV storage systems. PV generation costs compete with the retail price of electricity instead of the generation costs of other power sources when deployed on buildings (Lang et al. 2016).

The analysis of PV self-consumption in existing studies has mainly focused on case-building types, such as single houses (Hoppmann et al. 2014; Lang et al. 2015), small scale residential (Castillo-Cagigal et al. 2011), apartments (Fina et al. 2021; Boussaa et al. 2023), large offices (Perez et al. 2003), or university campuses (Glassmire et al. 2012). Duman and Güler (2020) used the HOMER grid to simulate the rooftop PV power generation of 5 kW grid-connected houses in nine Turkish provinces under the current feed-in tariff (FiT) scheme and conducted an economic analysis. Lang et al. (2015) used the HOMER grid to analyze the potential of PV self-absorption of four different building types (residential and commercial, large and small) in Germany, Switzerland, and Austria. They discussed the diffusion barriers, namely mechanisms that hinder market adoption of cost-effectiveness, such as split incentives and risk and uncertainty. Emmanuel et al. (2017) evaluated the performance analysis and economic feasibility of a 10 kW grid-connected solar PV system installed at the Maungaraki School in Wellington under the "Dynamics Project" in New Zealand. At an 8% discount rate, its normalized energy cost is 16.2 c/kWh, and the simple payback period is 6.4 years. The total electricity the grid consumes has decreased significantly by 32% yearly. In terms of currency, schools have effectively cut their electricity bills by 45%, saving about NZ $4,700 in 2014. Anagnostopoulos et al. (2017) analyzed the impact of feed-in tariff reduction on the payback period, internal rate of return, and profitability index of residential rooftop PV systems. When the cost of PV power generation is lower than the grid price, self-consumption reduces the electricity bill of the building, creating monetary value without subsidies.

The production cost of energy determines its economic competitiveness (Ren et al. 2018b). Research shows that technological advancements tend to decrease the price of PV modules, thereby significantly reducing initial investment costs (Fu et al. 2016; Liu and Tan 2016). El-Shimy et al. (2009) presented a viability analysis of a 10 MWp grid-connected PV plant for 29 different sites in Egypt. The energy production cost ranged from $0.1989/kWh to $0.2424/kWh, and the equity payback varied between 4.9 years and 7.1 years. Also, continuous technological progress reduces the cost of initial investment and operation and maintenance (O&M) processes (Obi et al. 2017). Over the years, the increased cost competitiveness of solar PV systems continues to drive them as a viable alternative to power generation in the global energy portfolio (Emmanuel et al. 2017).

At the same time, solar radiation is time-, location- and condition-dependent, and shadows cast on surfaces by buildings, vegetation, or structural elements make shading analysis necessary (Freitas et al. 2015). Li et al. (2015) studied the solar potential of urban residential buildings and found different effects of building plane form, building azimuth, and site coverage on PV and ST yields under low, medium, and high-density scenarios. Hong et al. (2017) studied the solar power utilization potential in southern parts of Seoul and estimated the entire block's overall solar power utilization potential. They found that the impact of block shadowing on solar power utilization potential is significant under real street conditions. Xu et al. (2021) used typical high-density blocks to quantitatively evaluate the differences in building rooftop shadowing caused by urban blocks and building functions. The linear regression algorithm was used to analyze the land use index (building density) and obtain the rooftop solar energy utilization potential prediction curve in Wuhan. The blocking coefficients were finally obtained by comparing the curve with it under no shadowing. The overall roof shadowing coefficient in Wuhan was 0.079, and the solar potential of Hengshan County in Wuhan was calculated, with a PV energy production capacity of 168.02 GWh per year. Kanters et al. (2014) used Ecotect simulation software to study the effects of urban density, building area, building area ratio, and direction on solar potential. Their results showed that if the design is inappropriate, solar potential can decrease by 10%–75%. Mohajeri et al. (2016) analyzed the impact of urban compactness on solar potential in 16 communities in Geneva. Their

results showed a high increase in solar radiation from compact to scattered communities, with a maximum rise of 30%–40% per year.

According to the above research, there are still defects in evaluating the economic benefits of the rooftop PV industry. First, the current subsidy policy differs from the past, while the existing research only analyzed the past subsidy policy, with the lack of building PV since the given potential exploration. Since the given ability is affected by local solar energy resources and price policies in different regions, the current research city is more concentrated in several typical cities. Therefore, this paper aims at the above issues and conducts a study mainly with the following objectives: (1) identify the PV self-consumption potential of industrial and commercial users in 20 regions of China; (2) explore the impact of electric prices and shading conditions on the system's feasibility; (3) provide advice for companies and policymakers to develop rooftop PV deployment. Economic indicators such as net present value（NPV）, internal rate of return (IRR), and investment payback period are selected to build an evaluation system to evaluate the economic performance of the investment projects in each region. The above indicators, NPV and IRR, were chosen to assess the convenience of PV investment, and this study used the investment payback periods to measure the speed of the recovery of the power generation industry.

2 Methods

This paper investigates the economics of rooftop PV systems under different shadowing conditions for 20 cities in China. Firstly, the architectural building models were constructed by QGIS and output the GeoJSON data. GeoJSON is a format for encoding data about geographic features using JavaScript Object Notation (JSON). The EnergyPlus building models were then generated by the City Buildings, Energy, and Sustainability (CityBES) platform to predict the power generation potential of buildings in 20 cities under no, medium, and high shadowing conditions. Finally, according to the investigation results of the rooftop PV system construction cost and investment return index, the economic performance analysis model was constructed considering the time value of the capital and electricity prices. The specific economic analysis indicators include static investment payback period (Pt) and dynamic investment payback period (P't), net present value (NPV), and internal rate of return (IRR). Figure 1 shows the overall workflow of this study.

2.1 Energy building models

2.1.1 20 typical representative cities

China has a vast territory and uneven distribution of solar energy resources. The total annual solar radiation is 3340–8400 MJ/m^2, and the median value is 5852 MJ/m^2 (CPIA 2022). This study selected 20 typical representative cities in China as the analysis GB50178-93 (MOHURD 1993). The specific zones are shown in Table 1. The CSWD of Chinese standard-year meteorological data obtained from EnergyPlus's official meteorological data center was used as weather documents.

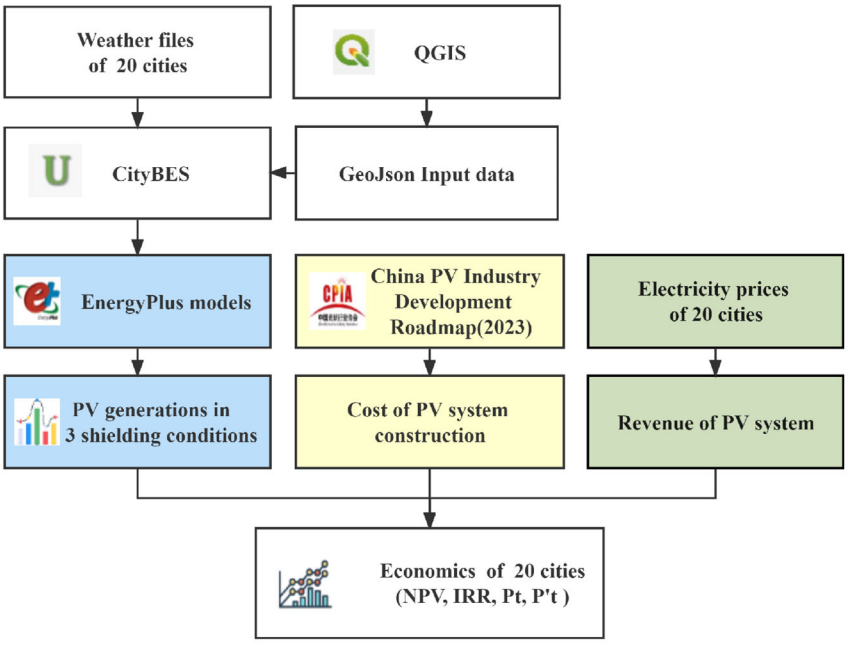

Fig. 1 The overall workflow of the study

Table 1 Geographical coordinates of the regions

City	Province/Autonomous region/Municipality	Latitude (°N)	Longitude (°E)	Solar energy resource area	Climatic regions
Shenzhen	Guangdong	22.32	114.08	III	Hot summer and warm winter (HW)
Zhangzhou	Fujian	23.80	117.66	III	
Shanghai	Shanghai	30.40	121.51	III	Hot summer and cold winter (HC)
Changsha	Hunan	28.12	112.59	III	
Chengdu	Sichuan	30.40	104.06	IV	
Guiyang	Guizhou	26.35	106.42	IV	Mild (M)
Kunming	Yunnan	25.04	102.71	II	
Beijing	Beijing	30.35	116.25	II	Cold (C)
Kashi	Xinjiang	39.55	75.99	I	
Taiyuan	Shanxi	39.47	112.54	II	
Lhasa	Tibet	37.54	91.13	I	
Ejin. Qi	Inner Mongolia	29.39	101.06	I	Severe cold (SC)
Shenyang	Liaoning	39.52	123.42	II	
Urumqi	Xinjiang	41.48	87.62	I	
Xining	Qinghai	43.45	101.77	I	
Karamay	Xinjiang	36.38	84.87	I	
Harbin	Heilongjiang	45.30	126.64	II	
Nenjiang	Heilongjiang	45.44	125.22	II	
Mohe	Heilongjiang	49.17	122.53	II	
Madoi	Qinghai	53.48	98.21	I	

2.1.2 Building models

Urban building energy models (UBEM) are valuable tools for city managers to assess and prioritize energy conservation measures (ECMs) for investment and design incentive and rebate programs. In this study, the CityBES was utilized to construct an EnergyPlus model for the building and evaluate rooftop PV power generation potential under three conditions: no shadowing, moderate shadowing, and high shadowing.

CityBES is an open web-based tool designed to aid in developing city-wide building energy efficiency strategic plans and programs. It can analyze the rooftop PV power generation potential for a building complex. It can export an EnergyPlus model, a 3D model that considers the shadowing effects of surrounding buildings. The specific building information includes building ID, height, and contour area (Chen et al. 2017). At the same time, Commercial Building Energy Saver (CBES) outputs the simulation results of PV modules, including PV annual generation strength and PV annual generation potential. For the city GIS dataset, GIS-based building footprint, year of construction, building type, building height, and the number of stories are necessary data elements that must be in GeoJSON or CityGML formats (Chen et al. 2017). The GeoJson input data was obtained in this study by the geoinformation tool QGIS.

Furthermore, the generation of PV systems is greatly affected by shadows. The amount of solar radiation depends on time, location, and conditions, and the shadows cast by buildings, foliage, or other structural elements on the surface make it necessary to perform obstacle analysis. The sunshine environment in the city, especially the roof sunshine, is complex, and the main reason is the number of high-rise buildings. With the increase in building density, the roofs of the ground and low-story buildings are seriously blocked. As such, it is essential to consider the potential impact of building shadows on PV system performance.

Table 2 shows the specific parameters of the basic building model. This study chose the mall as the typical building type. The rooftop areas of malls are typically large but easily occluded for the complex form of the surrounding buildings and the low height of itself. And malls have a significant volume and concentrated load demand. Furthermore, commercial and industrial users must pay for

Table 2 Parameters of the basic building

Parameter	Unit	Numerical value
Length	m	80
Width	m	35
High	m	20
Floor	—	5
Roof area	m^2	2800

higher electricity prices, which can further reduce electricity costs and increase overall economic benefits. The total number of floors is 20 m, belonging to the multi-story building. According to the standard GB 50352-2019 (MOHURD 2019), the spacing between multi-story buildings and high-rise buildings is 12 m at last. As shown in Figure 2, this study defined three kinds of shadowing as below:

1) No shadowing: the surrounding buildings are below or equal to the target building;
2) Medium shadowing: the surrounding buildings are 16 floors, 50 m;
3) High shadowing: the surrounding buildings are 25 floors, 75 m.

The front and rear building spacing (D) was determined by calculating the minimum spacing distance, as shown in Equation (1). And the minimum spacing distance is to ensure that the rear house can get no less than one hour of full window sunshine on the ground floor of the winter solstice, as shown in Figure 3.

$$D = H \times \cot(90 - 23.36 - L) \quad (1)$$

where: D is the distance between the basic building and the front and rear building (m), H is the height of the front and rear buildings (m), L is the local latitude of each city (°), and 23.36 is the solar angle at noon on the winter solstice (°).

2.1.3 *Rooftop PV system*

The solar PV power generation efficiency is mainly affected by the energy efficiency of PV modules, the installation method of PV modules (azimuth angle, square array spacing, inclination angle), and climatic conditions. PV panel orientation is commonly set to the south to maximize solar energy capture. When the inclination angle of the solar array is the same as the local latitude, most solar energy can be obtained throughout the year (Labed and Lorenzo 2004; Akinyele et al. 2015). Therefore, in this study, the orientation of the PV modules on the roof is set to the south direction, and the inclination angle is kept the same with the latitude in different regions. Table 3 shows the parameters of a PV module used in this paper.

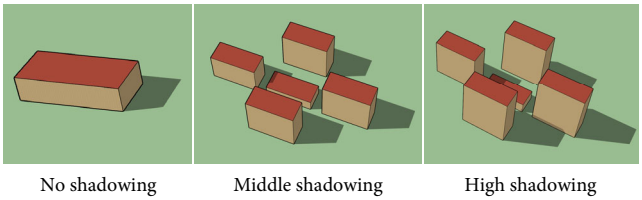

Fig. 2 Building models under three shadowing conditions

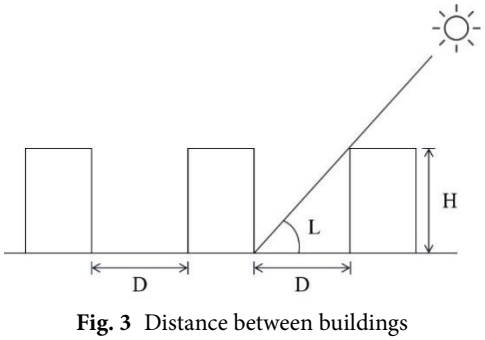

Fig. 3 Distance between buildings

According to the standard of the Code for Design of PV Power Plants (GB50797-2012) (MOHURD 2012), it is necessary to ensure that the front, back, left and right are not blocked from each other during 9:00–15:00 (local apparent sun) of the year. As shown in Figure 4, the array interval of the PV system (D_{PV}) can be calculated by the height of the PV system in front (height of shelter) (H_{PV}), as shown in Equation (2).

$$D_{PV}/H_{PV} = \cos\gamma/\tan\alpha \quad (2)$$

where: α is the solar elevation (°), γ is the solar azimuth (°).

2.2 Case study

This paper assumed the same PV system (the actual PV area is 100 m^2), and the cost of the system is shown in Table 4.

Table 3 Main technical parameters of PV modules

Parameter	Unit	Numerical value
Cell type	—	Poly crystalline silicon
The active area of the PV module	m^2	1.05
Module efficiency	%	13.7
Tilt angle from horizontal	degree	Latitude of different regions
Open circuit voltage	V	36.4
Short circuit current	A	8.3
Operating Voltage	V	30
Working current	A	7.5
Number of cells on a PV module	Piece	60
Nominal operating cell temperature test ambient temperature	°C	20
Nominal operating cell temperature test cell temperature	°C	47
Nominal operating cell temperature test insolation	W/m^2	800

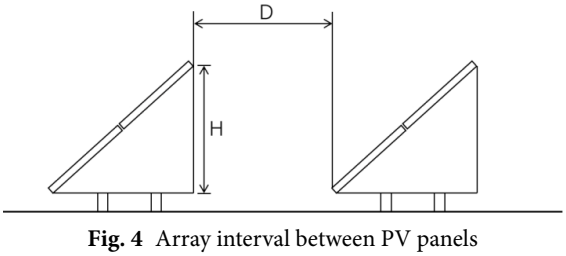

Fig. 4 Array interval between PV panels

Table 4 Parameters of case rooftop PV system

Parameter	Unit	Numerical value
Single PV panel power	kW	0.225
Number of PV panels	Piece	60
Number of vertical	Piece	6
Number of lateral	Piece	10
PV panel size	mm	1.64 × 0.99
Installed capacity	kW	13.5
Construction cost	RMB	46200
Construction period	Year	0.5
Operation cycle	Year	20
Operating costs	RMB/(W·Year)	0.04
Annual discount rate *i*	%	5

Note: Assuming that the life cycle of a PV system is 20 years, the efficiency of a PV system will decrease to 97% after one year, and the remaining years of the first decade will be calculated by averaging 10% to 3%. The annual efficiency decrease rate after the first decade is 1%.

And the electricity price income shall be calculated according to 90% of the electricity purchase price (Camilo et al. 2017).

2.3 Cost and revenues

The expenses of the power generation industry (TLC) can be divided into construction cost expenditures (PC_k), operating and maintenance expenses (PC_{om}), and fuel expenses (PC_{fuel}) throughout their entire life cycle (Ren et al. 2018a), as shown in Equation (3). Since rooftop PV power stations do not require fuel, there is no fuel expenditure. The total expenses include capital expenditures and operating and maintenance expenses (PC_{om}), which is the annual expenditure of rooftop PV power stations during their lifespan (Korsavi et al. 2018; Zhao and Xie 2019). Among them, construction cost expenditures (PC_k) calculation is closely related to the production cycle. In addition, the construction cycle of rooftop PV power stations is usually less than one year (Zhang et al. 2015).

$$TLC_{PV} = PC_k + PC_{om} + PC_{fuel} \quad (3)$$

2.3.1 *Initial total investment of rooftop PV systems*

The most significant cost items to set up a solar PV power station include the following: the PV module costs (40%–55% of the total amount), the inverter/cable/protection costs (10%), the building-integration costs (10%–15%), the installation costs (10%–15%), the design/bureaucratic-document costs (5%–10%) (Li et al. 2018).

According to the China PV Industry Development Roadmap (2022) (CPIA 2022), as shown in Figure 5, the initial total investment (CAPEX) of industrial and commercial distributed PV systems in China mainly consists the CAPEX of modules, inverters, supports, cables, construction and installation costs, grid access, roof leasing, roof reinforcement, and primary and secondary equipment. The primary equipment includes the box-type transformer, switch box, and prefabricated cabin. The CAPEX of industrial and commercial distributed PV systems in China is 3.74 RMB/W in 2021 and is expected to drop to 3.53 RMB/W in 2022.

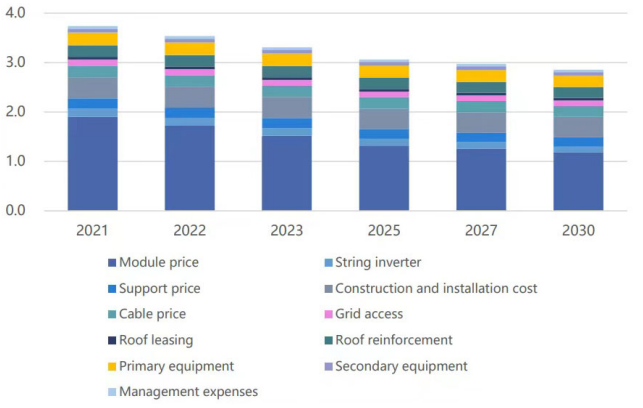

Fig. 5 Change trend of initial total investment (CAPEX) of industrial and commercial distributed PV systems in China between 2022 and 2030 (in RMB/W) (CPIA 2022)

2.3.2 *Operation and maintenance cost of the power station*

Power station operations are based on scientific and reasonable management of the power station, such as preventive maintenance, periodic maintenance, and regular equipment performance tests, to ensure the stable and efficient operation of the whole power station PV power generation system. It also ensures investors' returns and is the basis of power station trading and refinancing.

According to the China PV Industry Development Roadmap (2022) (CPIA 2022), from which this study has collected relevant data and shown in Figure 6, the operation and maintenance cost (YCF) of the distributed PV system is 0.051 RMB/(W·year) in 2021, and that of the centralized ground power station is 0.045 RMB/(W·year), slightly lower than those in 2020. It is expected that the operation

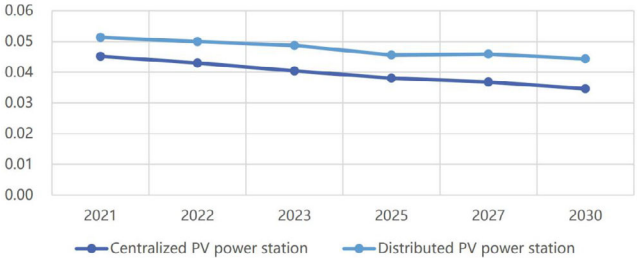

Fig. 6 Change trend of operation and maintenance costs (YCF) of PV power stations in China between 2021 and 2030 (in RMB/(W·year)) (CPIA 2022)

and maintenance costs of ground PV power stations and distributed systems will continue to remain at this level and decrease slightly in the next few years.

2.3.3 Total revenues

The income of rooftop PV power stations in the whole life cycle (TLR_{PV}), in which annual generation income (NP_{PV}) is determined by the annual generation and electricity price (Ren et al. 2018a), as shown in Equation (4).

$$NR_{PV} = E_i \times \pi \times P_{ei1} + E_i \times (1-\pi) \times P_{ei0} \quad (4)$$

where: E_i is the annual PV power generation (kWh/m^2), P_{ei0} is the feed-in tariff (including subsidies) (RMB/kWh), P_{ei1} is the self-use electricity price (including subsidies) (RMB/kWh), NR_{PV} is the power-generating revenues per period (year), π is the ratio of self-use electricity (%).

This paper assumed that all the power generation of PV systems is for their use, and the saving amount is calculated according to the electricity purchase price of industrial and commercial users (general industry and commerce, less than 1 kV users in 2023).

2.4 Economic indicators

Financial analysts usually rely on several financial metrics, such as the net present value (NPV) and the internal rate of return (IRR), to evaluate the convenience of an investment in electricity production or any other project. These two measures are commonly used as indicators of the profitability and feasibility of the project over its lifetime (Hoppmann et al. 2014). The profitability of the rooftop PV investment of this study was evaluated through the definition of different economic indicators: fixed payback period (Pt), dynamic payback period (P't), net present value (NPV), and internal rate of return (IRR).

2.4.1 Net present value

Net present value (NPV) is usually used to represent the size of annual earnings and is a basic indicator to evaluate the economic performance of a project (Lee 2016; Ren et al. 2018a). If the NPV of a project is positive, it indicates that the project can recycle investment, and the larger the NPV, the earlier the investment costs will be recycled, with the faster return on investment. The equation for calculating NPV is shown in Equation (5).

$$NPV = -CAPEX + \sum_{n=1}^{N} \frac{YCF}{(1+i)^n} \quad (5)$$

where: N is the technical lifetime of the PV plant, i is the discount rate to actualize cash flows at any given year (%).

The equations for calculating CAPEX and YCF are shown as Equations (6) and (7).

$$CAPEX = CAPEX_{PV} \times P_{PV;m^2} \quad (6)$$

$$YCF = YCF_{PV} \times P_{PV;m^2} \quad (7)$$

where: $P_{PV;m^2}$ is the ratio between the PV system's peak power and the PV modules' general area A (kW/m^2), $CAPEX_{PV}$ is the per unit initial cost of the PV system (RMB/kW), YCF_{PV} is the per unit yearly operational cost of PV peak power (RMB/kW).

2.4.2 Internal rate of return

Internal rate of return (IRR) is a financial indicator used to measure the potential return on investment and determine whether it is worthwhile. In the rooftop PV industry, the IRR reflects the investment return on the entire year's initial construction costs (Ramírez-Sagner et al. 2017; Zhao and Xie 2019).

The feasibility of a PV project can be determined by comparing the value of IRR and i: firstly, a benchmark discount rate (i_0) was chosen and compared with the internal rate of return finally. If the internal rate of return is greater than or equal to the benchmark discount rate, it indicates that the user or investor has good debt-paying ability and that the PV project is feasible. On the other hand, if the internal rate of return is less than the benchmark discount rate, the PV project is not feasible. And the equations for calculating IRR are shown in Equations (8) and (9).

$$\sum_{t=0}^{n} \frac{C_t}{(1+i)^t} = 0 \quad (8)$$

$$IRR = i \quad (9)$$

where: C_t is the net cash flow in year t (RMB), n is the life of the project (year), i is the internal rate of return (%).

2.4.3 Investment payback period

The payback period reflects the project's income, which is used to measure the speed of the recovery. Static investment recovery period (denoted by Pt in this article) refers to a method of determining the recovery period of an investment without considering interest costs, directly comparing the net present value of the investment project with the initial investment, and thus establishing the recovery period. It should be noted that Pt is just a simple indicator and cannot reflect the impact of intangibility costs such as inflation or currency devaluation.

The dynamic investment payback period (denoted by P't in this article) overcomes the disadvantage of the static investment payback period without considering the time

value of capital (Sun et al. 2018). Specifically, in the calculation process of the dynamic investment recovery period, it needs to consider the investment costs of the project, expected returns, inflation rates, currency devaluation rates, and other factors, and then use these factors to calculate the dynamic investment recovery period of the project. Pt and P't can be calculated by the same equation, as shown in Equation (10).

$$P = T - 1 + \frac{\left|\sum_{n=1}^{T-1}(\mathrm{CI}-\mathrm{CO})_n\right|}{(\mathrm{CI}-\mathrm{CO})_T} \tag{10}$$

where: T is the number of years when the accumulated cash flow is positive or zero for the first time, CI is the annual cash inflow (RMB), CO is the annual cash outflow (RMB). The CO of the first year is the initial investment cost and the subsequent years are maintenance costs.

3 Results

3.1 Yearly PV production

Based on geographical locations, six cities were selected (Harbin, Beijing, Kashi, Shanghai, Zhangzhou, and Chengdu), and their PV system monthly electricity production was analyzed, as shown in Figure 7. Due to the influence of temperature effects and weather conditions, the peak of PV power generation in northern cities does not occur during the summer, which has the best sunlight conditions. Harbin and Beijing have similar latitudes, and the maximum electricity production was observed in March (37.52 kW and 34.84 kW), while the minimum was followed in December (21.11 kW and 24.19 kW). Overall, the PV system performance in the north city was more variable due to weather effects, and the monthly average electricity production was relatively higher in spring compared to other seasons. In the southern regions, such as Shanghai, the PV system performance is more consistent, with better performance in summer than in winter. The maximum monthly electricity production was observed from May to August, while the minimum was from December to February.

Figure 8 shows the annual power generation per PV power unit in 20 cities without shadowing. Among them, the annual output of PV systems in Kashi is the highest at 233.99 kWh/m^2, while Chengdu has the lowest at 84.14 kWh/m^2. The annual PV power generation value in regions with high latitudes and altitudes in the northwest and north, which belong to areas rich in solar energy resources, can reach more than 200 kWh/m^2. The average annual electricity generation per unit PV area in the southern region is 121.71 kWh/m^2; in the northern region, it can reach up to 189.72 kWh/m^2. This is due to the relatively low latitude and shorter sunshine hours in southern regions and the frequent occurrence of cloudy and rainy weather conditions, resulting in unstable solar irradiance. The difference in altitude between regions also affects the performance of PV systems. Generally, higher altitudes are associated with lower temperatures. Since the efficiency of solar cells decreases with increasing temperatures, PV systems in high-altitude areas may have higher electricity generation efficiency.

Additionally, high-altitude areas often experience more sunshine hours and less cloud cover. These climatic conditions are favorable for the efficiency and output of PV systems. For example, in Chengdu and Guiyang in the southwestern basin, the annual PV power generation value can only reach 85. In the southwest city of Lhasa, located on the Qinghai–Tibet Plateau, the yearly PV power generation can reach 189.17 kWh/m^2.

Figure 9 illustrates the annual changes in power generation under medium and high shadowing conditions. In the medium shadowing scenario, the height of the surrounding buildings is relatively low, and even when the building separation distance is large, the impact of building shadowing on the PV system remains relatively small. But, the variation in PV power generation among cities is insignificant, with a concentrated decrease in power generation ranging from 10% to 15%. However, in the high shadowing situation, the height of the surrounding buildings significantly exceeds that of the research buildings, resulting in extensive shadowing

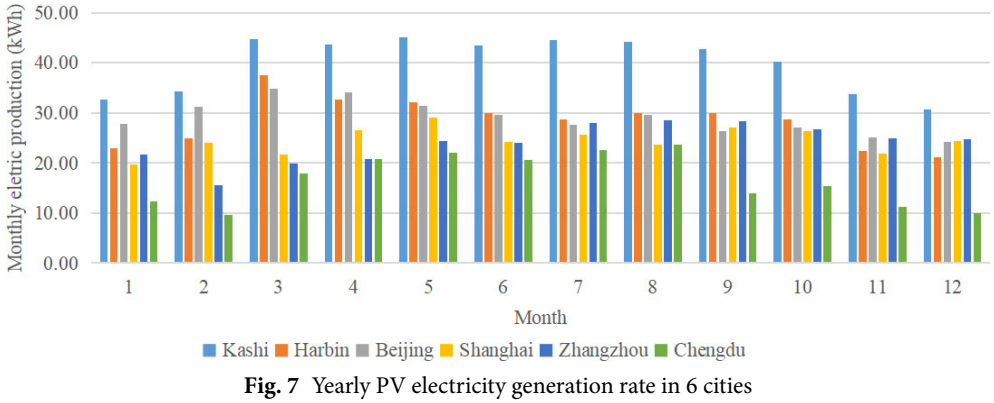

Fig. 7 Yearly PV electricity generation rate in 6 cities

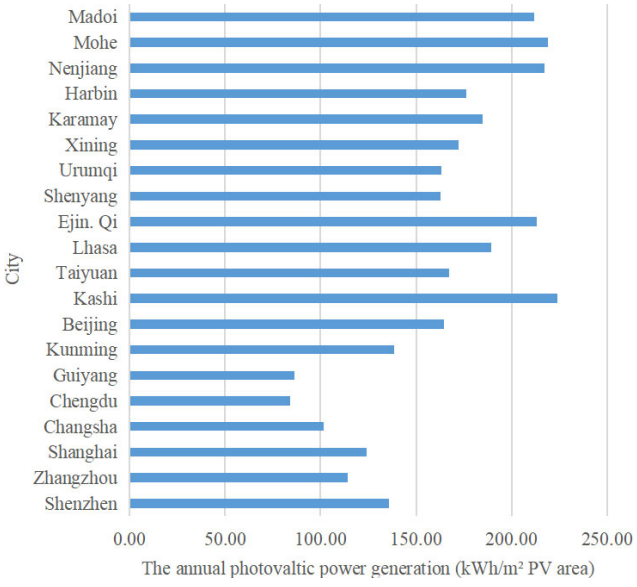

Fig. 8 Annual power generation per PV area of 20 cities without shadowing

of the PV system. Most cities experience a 37.02% decrease in PV power generation. However, in a few high-latitude regions like Karamay, where the building separation distance is larger, the impact of shadowing is relatively lower, with a decrease in PV power generation of around 30.13%. Particularly in Mohe, where the building separation distance reaches 85 m, the reduction in PV power generation is only 24.45%.

Figure 10 depicts the needed rooftop areas of the PV systems arranged of 20 cities. In this study, the arrangement of PV panels in 20 cities was all set in 10 rows and 6 columns, with no gaps between the horizontal arrays. Therefore, the vertical spacing between the panels, preventing self-shading, has the most notable effect on the required roof area. The needed rooftop area of 20 cities typically ranges from 100–200 m² in most cities. The minimum required rooftop area among 20 cities is Shenzhen, only 133.8 m². The compact arrangement of PV panels in southern cities reduces the wastage of rooftop space, allowing users to choose a more optimal layout. It also maximizes the utilization of available solar radiation and enhances the system's efficiency in generating electricity. However, in higher latitudes like Mohe, the array interval can reach 15 m, resulting in an area of 800 m². A comparison reveals that cities in high

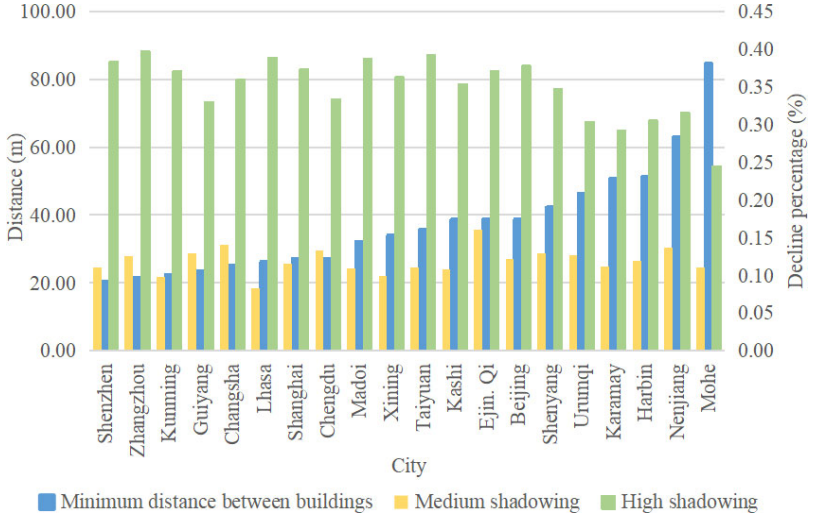

Fig. 9 The PV annual power generation changes under shadowing condition

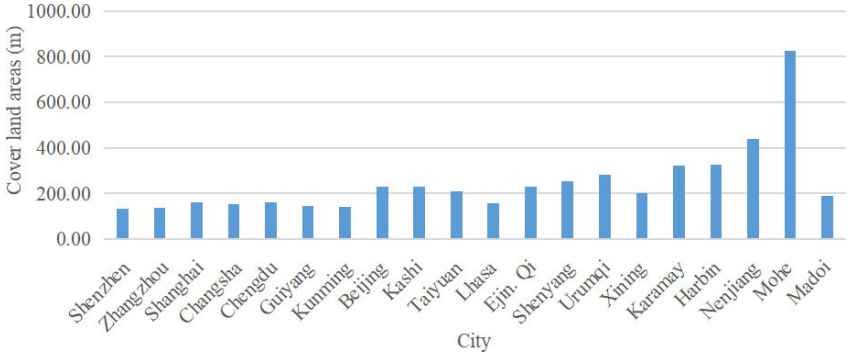

Fig. 10 Needed rooftop areas of the PV system

latitudes require a large roof area for installing rooftop PV systems with high installed capacity, making them more suitable for large-scale factories.

3.2 Economic analysis

Figure 11 shows the changes in the payback period among cities under three shadowing conditions. When the PV power generation is fully self-sufficient, most cities can recover their investment within 5–10 years under medium and no shadowing conditions, and even under high shadowing conditions, the dynamic payback period is around 15 years. A few cities have a better economic advantage, and the payback period is concentrated within 5 years in all three conditions. Figure 12 and Figure 13 present the NPV and IRR of rooftop PV systems in 20 cities in China. Zhangzhou, Guiyang, Urumqi, and Karamay have the lowest NPV and IRR values among these cities. Under the condition of no shadowing, the IRR of these cities, except Guiyang, can exceed the benchmark return rate (5%). The three cities in Heilongjiang have the best economic performance, while the IRR of cities in Xinjiang, also in the high latitude region, can barely reach 5% and realize the return. The NPV of Guiyang is −7298.1 RMB, and the IRR is 2.48% under no shadowing. Guiyang is the only city in China with a negative NPV and cannot reach the benchmark return under no shadowing. Compared with the cities in the same latitude belt, Guiyang has a poorer PV potential, and a single electricity price system is applied to low-capacity users, resulting in low electricity prices, which leads to low profits. Therefore, building rooftop PV systems for user self-consumption is challenging to recoup the returns.

Table 5 compares the cities with the longest and shortest payback periods, Mohe and Guiyang. The payback period of Mohe and Guiyang does not change much under medium shadowing, with static payback periods Pt increasing by 1.7 years and 0.4 years, respectively. However, under high shadowing conditions, the static payback period of Guiyang increased by 6.7 years compared to no shadowing, while that of Mohe only increased by one year. This is because Mohe has a high local latitude, and the distance between buildings reached 84.6 m, so the impact of surrounding

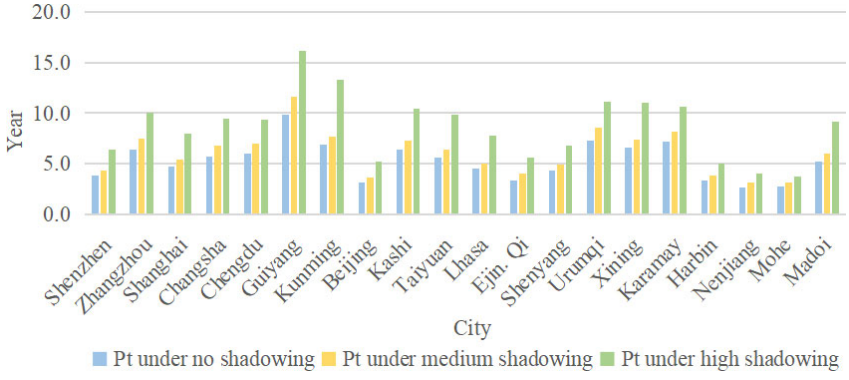

(a) Static investment payback period

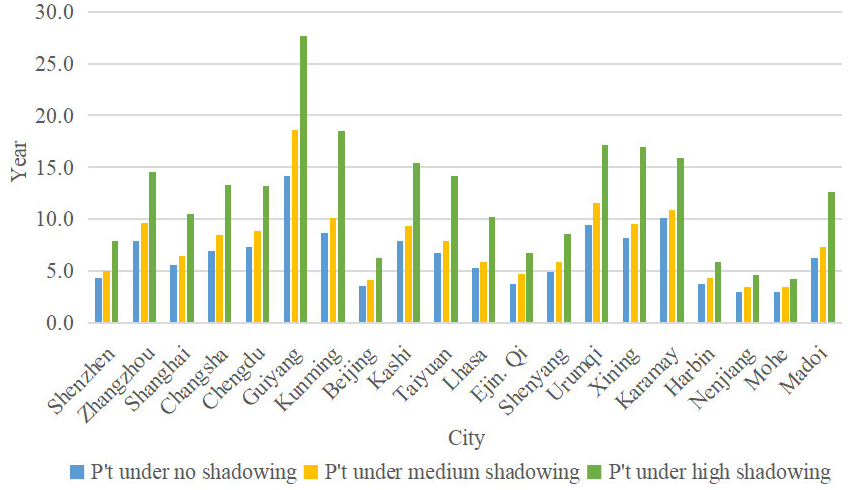

(b) Dynamic investment payback period

Fig. 11 The investment payback period of 20 cities

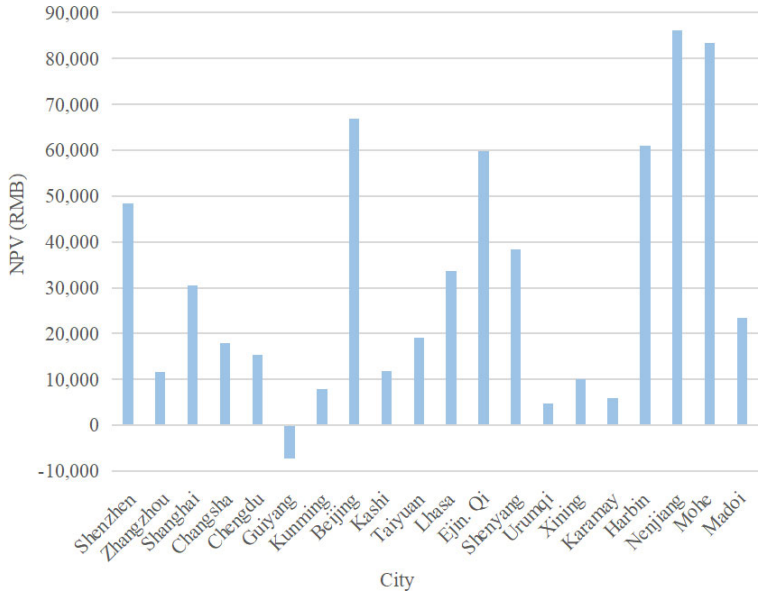

Fig. 12 The NPV of 20 cities under no shadowing condition

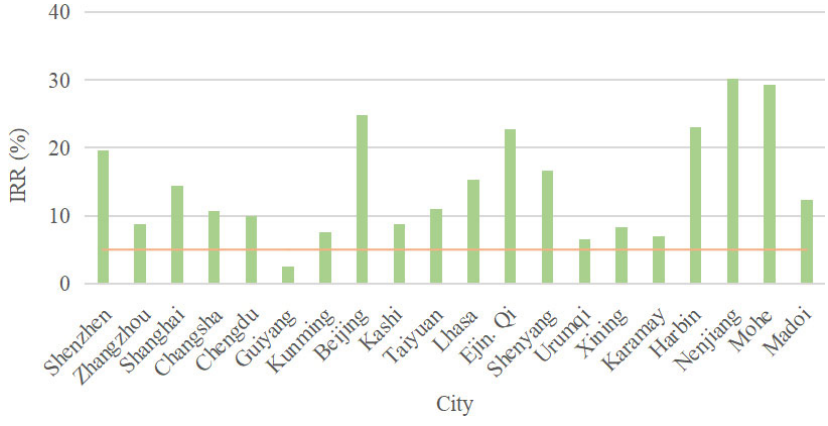

Fig. 13 The IRR of 20 cities under no shadowing condition

Table 5 Comparison of the investment payback period of Guiyang and Mohe

City	Shadowing condition	Price (RMB/kWh)				Annual PV electricity generation (kWh)	Pt (year)
		Spike	Peak	Usual	Trough		
Guiyang	No	0.7122				8650.69	9.5
	Medium					7530.03	11.2
	High					5794.00	16.2
Mohe	No	1.4275	1.1420	0.7696	0.3972	21888.84	2.72
	Medium					19464.42	3.09
	High					16537.31	3.67

buildings on Mohe is much smaller than that of on Guiyang under high shadowing. At the same time, compared to Guiyang, which implements a single electricity price, Mohe's basic electricity price is higher.

The distribution of electricity price periods in different provinces/autonomous regions/municipalities can be roughly classified into three categories, as shown in Figure 14: Category I has peak periods in the morning and evening, with peak or off-peak periods during noon and afternoon. Among the provinces/autonomous regions/municipalities included in this category, Xinjiang has the lowest price. Category II has peak periods in the morning and afternoon, with peak and off-peak periods occurring during noon and night. Among the provinces/autonomous regions/

municipalities included in Category II, Guangdong has the highest electricity price difference between peak and off-peak periods. Category III has a relatively even distribution of periods, with slight differences in electricity prices. The peak generation periods for PV systems are mainly during noon and afternoon, which coincide with the electricity price policy distribution in Category II. Therefore, cities that adopt the Category II electricity price policy, such as Shenzhen, show better economic performance. Cities that adopt the Category I electricity price policy are more suitable for implementing distributed PV systems with energy storage strategies. This allows the excess electricity generated during the day to be stored and used during high-price periods, thereby reducing users' costs. In provinces/autonomous regions/municipalities with Category III electricity price policies, such as Hunan with more off-peak periods and Tibet with a small difference in peak and off-peak prices (only 0.04), the electricity price policies set for large industrial users have greater fluctuations and more specific period divisions. For example, in Shanghai, the peak electricity price for 10 kV large industrial users can reach 1.3010 RMB/kWh. Therefore, it is more feasible to construct large-scale distributed PV systems in these cities.

Figure 15 shows the daily electricity prices and PV system output in three cities on July 21st. The peak generation periods for solar power in Nenjiang and Chengdu are from 9:00 to 17:00. At the same time, Urumqi, located in the westernmost part of China, experiences peak solar power generation from 13:00 to 19:00. Urumqi is a region with abundant sunshine and significant PV potential. Still, the electricity price is the lowest in the provinces/autonomous regions/municipalities belonging to the 20 cities. Moreover, during the peak solar power generation period in Urumqi, the electricity price is in the off-peak period, which further leads to Urumqi's poorer economic performance. Therefore, policymakers and decision-makers in these regions must devise and implement effective incentive policies and subsidies that encourage the construction of rooftop PV systems.

The electricity price distribution curve in Nenjiang also

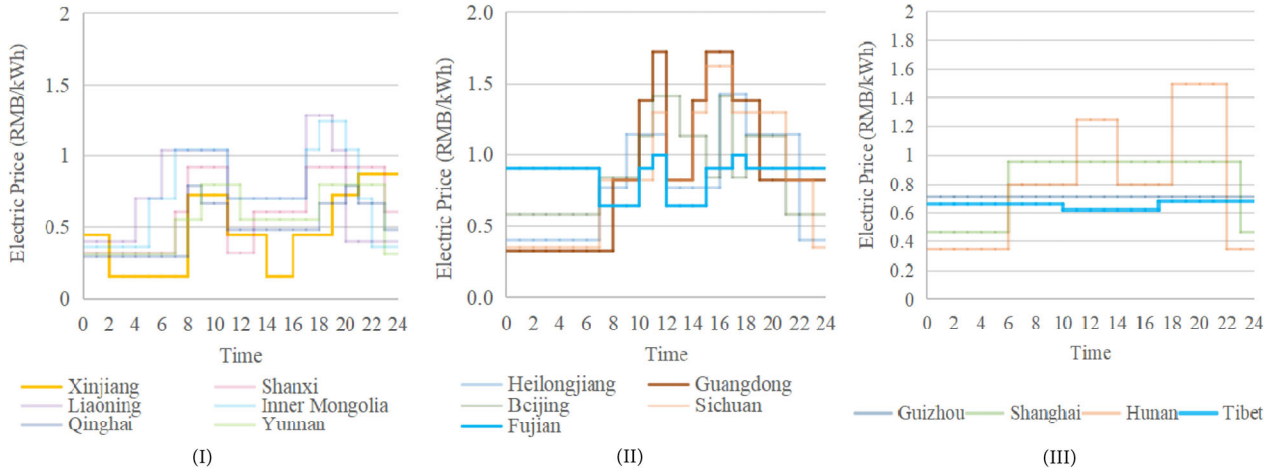

Fig. 14 Electricity price periods in different provinces/autonomous regions/municipalities

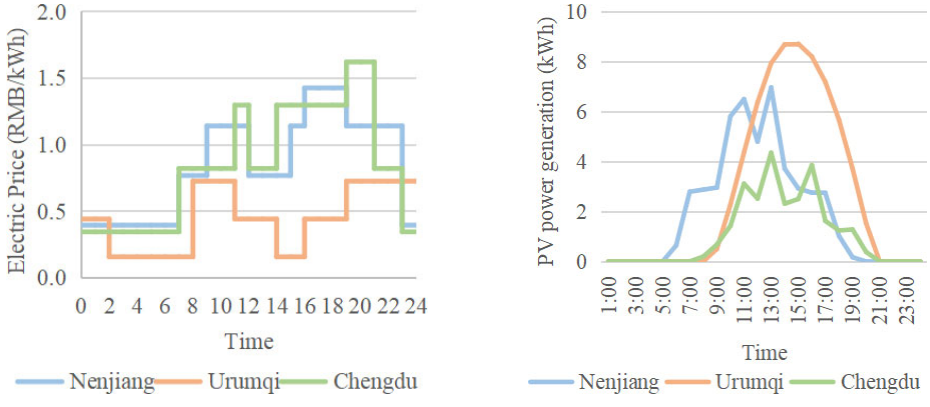

(a) Electricity price (b) Hourly PV generation under no shadowing

Fig. 15 Comparison of Nenjiang, Urumqi, and Chengdu

does not match the solar power generation curve. However, due to the abundant solar resources in Nenjiang, the annual PV generation reaches 217.49 kWh/(m^2 PV area). Additionally, Nenjiang has a relatively high benchmark electricity price. Therefore, it still maintains a higher level of economic viability. The influence of electricity prices on the economic performance of rooftop PV is also evident in the case of Chengdu. Although Chengdu has a relatively poor situation in terms of PV power generation, its peak electricity price period matches the PV generation curve and the electricity price is higher than the other cities. Therefore, under shadowing conditions, the economic performance of Chengdu is superior to that of Urumqi. However, when considering the factor of shadow, the capacity of PV power generation in Chengdu significantly decreases. When facing a high level of shadowing, the NPV is −5636.9 RMB, which means the investment cannot recover.

To explore the economic PV potential of Urumqi, this paper assumed that the electricity price during the same period in Urumqi is the same as that in Nenjiang, while the time-of-day distribution remains unchanged. Figure 16 compares the changes in various economic indicators of Urumqi with different electricity prices. Even if the timing of the electricity price policy is not changed, only increasing electricity prices, the financial performance of Urumqi has significantly improved. The static and dynamic investment payback periods have decreased considerably, and the dynamic investment payback period has reduced from 17 years to 9 years under high shadowing. Moreover, in all three shadowing cases, the NPV has achieved positive returns, and the IRR has exceeded the benchmark rate of return. A large amount of PV potential still exists under the existing costs and electricity prices, waiting to be developed in Xinjiang.

Table 6 displays the economic indicators of the 20 city-scale PV systems under three shadowing conditions. The impact of shadowing on PV electricity production reduces the economic efficiency of each city to varying degrees. In the absence of shadowing, except for Guiyang, all cities can exceed the benchmark return rate (5%). Among them, the cities of Heilongjiang and Beijing performed better economic efficiency. Most cities could achieve the benchmark return rate and financial profitability under medium shadowing conditions. However, only cities with high solar potential and electricity prices could achieve the benchmark return rate and financial profitability under high shadowing conditions.

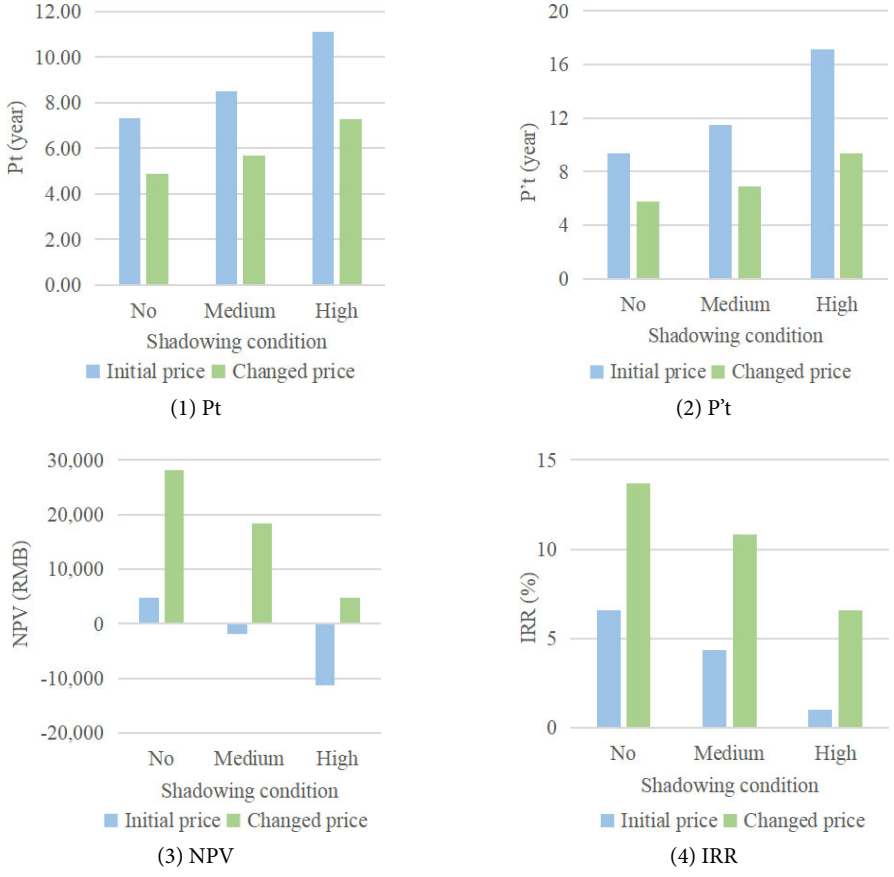

Fig. 16 Comparison of economic indicators after changing Urumqi electricity price

Table 6 Economic indicators of 20 cities under three shadowing conditions

	City	Annual PV electricity generation (kWh)	Annual revenue (RMB)	Pt (Year)	P't (Year)	NPV (RMB)	IRR (%)
No shadowing	Shenzhen	13579.37	13070.6	3.8	4.3	48357.3	19.54
	Zhangzhou	11430.23	8114.0	6.3	6.4	11701.6	8.76
	Shanghai	12396.87	10655.1	4.7	5.1	30493.8	14.40
	Changsha	10140.00	8956.3	5.7	5.9	17930.5	10.67
	Chengdu	8414.17	8611.2	5.9	6.0	15378.5	9.89
	Guiyang	8650.69	5518.4	9.5	14.0	−7298.1	2.48
	Kunming	13840.22	7589.9	6.8	6.5	7825.2	7.54
	Beijing	16446.12	15570.0	3.1	3.4	66841.1	24.75
	Kashi	22398.65	8119.6	6.3	6.4	11742.5	8.77
	Taiyuan	16723.19	9122.6	5.6	6.0	19160.2	11.04
	Lhasa	18916.53	11093.8	4.5	5.0	33737.8	15.35
	Ejin. Qi	21323.02	14625.2	3.3	3.6	59854.0	22.79
	Shenyang	16268.55	11716.1	4.2	4.5	38340.0	16.68
	Urumqi	16326.42	7181.3	7.2	6.3	4803.8	6.58
	Xining	17244.34	7887.5	6.5	6.3	10026.1	8.24
	Karamay	18468.91	7332.7	7.0	6.5	5923.5	6.94
	Harbin	17654.41	14778.5	3.3	3.7	60987.7	23.11
	Nenjiang	21749.66	18185.14	2.66	2.88	86181.15	30.14
	Mohe	21888.84	17801.90	2.72	2.96	83347.01	29.35
	Madoi	21168.80	9700.91	5.19	5.68	23437.12	12.32
Medium shadowing	Shenzhen	12078.06	11632.8	4.3	5.0	37724.4	16.50
	Zhangzhou	9993.67	7059.2	7.4	5.9	3900.8	6.28
	Shanghai	10970.77	9429.4	5.4	5.7	21429.0	11.72
	Changsha	8710.00	7702.4	6.7	6.8	8657.6	7.81
	Chengdu	7299.93	7491.8	6.9	6.7	7099.7	7.31
	Guiyang	7530.03	4803.5	11.2	18.6	−12781.0	0.45
	Kunming	12482.56	6845.3	7.6	5.8	2319.1	5.77
	Beijing	14437.48	13668.3	3.6	3.9	52777.8	20.79
	Kashi	19984.37	7226.4	7.2	6.1	5137.3	6.68
	Taiyuan	14868.68	8110.9	6.3	6.4	11678.7	8.75
	Lhasa	17348.18	10206.3	4.9	5.4	27174.4	13.43
	Ejin. Qi	17908.84	12283.4	4.0	4.4	42536.0	17.88
	Shenyang	14176.35	10209.3	4.9	5.4	27197.1	13.43
	Urumqi	14176.35	6274.4	8.4	11.5	−1902.8	4.36
	Xining	15537.13	7106.6	7.3	6.5	4251.3	6.40
	Karamay	16397.97	6510.5	8.0	10.8	−157.2	4.95
	Harbin	15540.77	13005.1	3.8	4.1	47872.6	19.40
	Nenjiang	18775.65	15698.53	3.12	3.37	67791.79	25.01
	Mohe	19464.42	15830.16	3.09	3.33	68765.19	25.29
	Madoi	18857.33	8633.81	5.89	6.37	15545.52	9.94

Table 6 Economic indicators of 20 cities under three shadowing conditions (Continued)

	City	Annual PV electricity generation (kWh)	Annual revenue (RMB)	Pt (Year)	P't (Year)	NPV (RMB)	IRR (%)
High shadowing	Shenzhen	8370.71	8103.8	6.4	7.9	11625.7	8.74
	Zhangzhou	6890.75	4868.4	9.9	14.5	−8232.3	2.13
	Shanghai	7770.80	6679.0	7.8	6.0	1089.0	5.36
	Changsha	6490.00	5732.0	9.2	13.3	−5914.2	2.97
	Chengdu	5608.61	5769.5	9.1	13.1	−5636.9	3.07
	Guiyang	5794.00	3696.1	16.2	27.7	−20970.9	0.12
	Kunming	8710.36	4308.1	13.3	18.5	−16444.5	0.33
	Beijing	10229.55	9684.6	5.2	5.7	23316.4	12.29
	Kashi	14478.20	5277.7	10.1	14.2	−9274.0	1.12
	Taiyuan	10164.77	5544.9	9.5	14.0	−7297.8	2.48
	Lhasa	11562.05	6767.2	7.7	6.2	1741.2	5.58
	Ejin. Qi	13404.92	9194.3	5.5	5.9	19690.3	11.20
	Shenyang	10624.69	7651.5	6.7	6.3	8281.3	7.69
	Urumqi	10624.69	4998.8	10.7	17.1	−11336.6	1.00
	Xining	10987.57	5025.7	10.6	15.1	−11138.1	1.08
	Karamay	13081.46	5193.7	10.3	15.8	−9895.1	1.54
	Harbin	12263.28	10197.2	4.9	5.5	27107.0	13.41
	Nenjiang	14884.76	12445.32	3.99	4.48	43733.03	18.22
	Mohe	16537.31	13449.58	3.67	4.02	51159.91	20.33
	Madoi	12960.16	5917.55	8.92	11.34	−4542.20	3.45

4 Discussion

Regarding the assessment of PV potential, Wang et al. (2017) conducted a study using a GIS platform to assess solar power generation potential in China. They found that annual mono crystalline-silicon PV power generation in the northwestern and northern regions can exceed 200 kWh/(m^2·year), while the potential in the southwestern areas is limited to around 130 kWh/(m^2·year). The findings from their research align with the simulation results obtained in this current study. But the solar power generation potential in the southwestern region of China is lower than that in the study by Wang et al. (2017) due to the utilization of dynamic weather files.

According to the standard of climatic regionalization for architecture, this study selected 20 typical cities for research and evaluated the economic potential of the rooftop PV industry in China. The results of this study indicate that rooftop PV systems in a self-consumption mode have become economically attractive in many cities, even without subsidy policies. In the absence of shading, most cities' static investment payback period ranges from 5 to 10 years, with the shortest period being as low as 2.66 years and the return rate reaching 30.14%. These findings provide valuable insights for commercial and industrial users considering investing in rooftop PV systems. However, building shadowing is a crucial driver of the profitability of rooftop PV systems. The static investment payback period can be extended from 9.5 to 16.2 years under high shadowing. Electricity prices also serve as a direct constraint on the development of rooftop PV, as observed in cities like Urumqi, where solar resources are abundant, but electricity prices are set low, with peak electricity prices occurring at night. Therefore, adopting energy storage systems to balance supply and demand may be feasible to enhance the economic viability of rooftop PV systems in similar regions and reduce energy costs. This consideration also presents one of the avenues for further exploration in future research to improve the economic feasibility of rooftop PV. Guiyang, another low-profit city, is in a poor solar resources area and has a single cheap electricity price for small-scale commercial users rather than the time-of-use price. The discounted income over the whole life cycle is 46197.9 RMB, less than the sum of the initial investment and O&M cost, resulting in a negative NPV. In such regions, utilizing more efficient PV modules and optimizing layout to avoid shadowing are crucial factors for improving the economic viability of rooftop PV systems.

There are limitations for the building layouts used in Figure 2. This paper tried to define different building shadowing conditions and preliminarily explored the specific impact of environmental shadow. Future studies will develop prototype building energy models with proper shadowing conditions based on detailed analysis of the GIS building datasets, which can help better estimate the PV potential of urban buildings. Additionally, although the cities in north China exhibit higher solar power generation potential, the weather conditions present challenges for the performance and maintenance of PV systems. Some emergencies, like low temperatures and snow, may not only lead to performance degradation but also necessitate more frequent surface cleaning of PV panels. Consequently, these challenges can increase operation and maintenance expenses, reducing economics.

5 Conclusions

Through the simulation and analysis of geographical and weather conditions, solar energy resources, building shadowing conditions, and subsidy policies, this paper explored the economic potential of building rooftop PV systems in 20 cities in China to provide a reference for the actual construction in each region. The findings of this paper are summarized as follows.

The average annual electricity generation per unit PV area in the southern region is 121.71 kWh/m^2; in northern cities, it can reach 189.72 kWh/m^2. Additionally, the efficiency of PV modules often decreases in summer due to high temperatures, high humidity and air pollution. So, the monthly maximum electricity generation of PV systems occurs in spring and autumn.

Regarding building shadowing, the annual electricity generation of PV systems decreased from 8.29% to 16.01%. However, the reduction will be amplified under high shading conditions from 24.45% to 39.71%. Due to increasing building spacing with latitude, some high-latitude cities experience a decrease of approximately 30.13% in PV electricity generation.

Matching electricity prices and peak/off-peak periods with the solar generation curve is advantageous. Nenjiang demonstrates the best economic performance among 20 cities, with high electricity prices and a good alignment between peak solar generation and peak electricity demand periods. Without considering shadowing effects, the investment payback period is 2.9 years, and the internal rate of return can reach 30.14%.

Overall, cities with high PV power generation potential, good alignment of electricity prices and peak/off-peak periods with solar generation, and considering shadowing factors have tremendous economic potential. This paper provides valuable insights into the economic feasibility of rooftop PV systems and can serve as a reference for policymakers and investors when assessing the viability of PV system construction in various regions across China.

Acknowledgements

This research was funded by Hunan University, China, through the start-up funds and the Course Development Program of "Artificial Intelligence in Built Environment".

Declaration of competing interest

The authors have no competing interests to declare that are relevant to the content of this article. Yixing Chen is a Subject Editor of *Building Simulation*.

References

Akinyele DO, Rayudu RK, Nair NKC (2015). Global progress in photovoltaic technologies and the scenario of development of solar panel plant and module performance estimation—Application in Nigeria. *Renewable and Sustainable Energy Reviews*, 48: 112–139.

Anagnostopoulos P, Spyridaki NA, Flamos A (2017). A "new-deal" for the development of photovoltaic investments in Greece? A parametric techno-economic assessment. *Energies*, 10: 1173.

Bazilian M, Onyeji I, Liebreich M, et al. (2013). Re-considering the economics of photovoltaic power. *Renewable Energy*, 53: 329–338.

Bergamasco L, Asinari P (2011). Scalable methodology for the photovoltaic solar energy potential assessment based on available roof surface area: Application to Piedmont Region (Italy). *Solar Energy*, 85: 1041–1055.

Boussaa Y, Dodoo A, Nguyen T, et al. (2023). Comprehensive renovation of a multi-apartment building in Sweden: techno-economic analysis with respect to different economic scenarios. *Building Research & Information*, https://doi.org/10.1080/09613218.2023.2240442

Camilo FM, Castro R, Almeida ME, et al. (2017). Economic assessment of residential PV systems with self-consumption and storage in Portugal. *Solar Energy*, 150: 353–362.

Castillo-Cagigal M, Caamaño-Martín E, Matallanas E, et al. (2011). PV self-consumption optimization with storage and Active DSM for the residential sector. *Solar Energy*, 85: 2338–2348.

Chen Y, Hong T, Piette MA (2017). Automatic generation and simulation of urban building energy models based on city datasets for city-scale building retrofit analysis. *Applied Energy*, 205: 323–335.

CPIA (2022). China PV Industry Development Roadmap. China Photovoltaic Industry Association.

Duman A, Güler Ö (2020). Economic analysis of grid-connected residential rooftop PV systems in Turkey. *Renewable Energy*, 148: 697–711.

EL-Shimy M (2009). Viability analysis of PV power plants in Egypt. *Renewable Energy*, 34: 2187–2196.

Emmanuel M, Akinyele D, Rayudu R (2017). Techno-economic analysis of a 10 kWp utility interactive photovoltaic system at Maungaraki school, Wellington, New Zealand. *Energy*, 120: 573–583.

Fina B, Roberts MB, Auer H, et al. (2021). Exogenous influences on deployment and profitability of photovoltaics for self-consumption in multi-apartment buildings in Australia and Austria. *Applied Energy*, 283: 116309.

Freitas S, Catita C, Redweik P, et al. (2015). Modelling solar potential in the urban environment: State-of-the-art review. *Renewable and Sustainable Energy Reviews*, 41: 915–931.

Fu R, Chung D, Lowder T, et al. (2016). U.S. Solar Photovoltaic System Cost Benchmark: Q1 2016. Technical Report, NREL/TP-6A20-66532. National Renewable Energy Laboratory (NREL).

Glassmire J, Komor P, Lilienthal P (2012). Electricity demand savings from distributed solar photovoltaics. *Energy Policy*, 51: 323–331.

Graebig M, Erdmann G, Röder S (2014). Assessment of residential battery systems (RBS): Profitability, perceived value proposition, and potential business models. Paper presented at the 37th IAEE International Conference, New York, USA.

Hong T, Lee M, Koo C, et al. (2017). Development of a method for estimating the rooftop solar photovoltaic (PV) potential by analyzing the available rooftop area using Hillshade analysis. *Applied Energy*, 194: 320–332.

Hoppmann J, Volland J, Schmidt TS, et al. (2014). The economic viability of battery storage for residential solar photovoltaic systems—A review and a simulation model. *Renewable and Sustainable Energy Reviews*, 39: 1101–1118.

Kanters J, Wall M, Dubois MC (2014). Typical values for active solar energy in urban planning. *Energy Procedia*, 48: 1607–1616.

Korsavi SS, Zomorodian ZS, Tahsildoost M (2018). Energy and economic performance of rooftop PV panels in the hot and dry climate of Iran. *Journal of Cleaner Production*, 174: 1204–1214.

Labed S, Lorenzo E (2004). The impact of solar radiation variability and data discrepancies on the design of PV systems. *Renewable Energy*, 29: 1007–1022.

Lang T, Gloerfeld E, Girod B (2015). Don't just follow the sun—A global assessment of economic performance for residential building photovoltaics. *Renewable and Sustainable Energy Reviews*, 42: 932–951.

Lang T, Ammann D, Girod B (2016). Profitability in absence of subsidies: A techno-economic analysis of rooftop photovoltaic self-consumption in residential and commercial buildings. *Renewable Energy*, 87: 77–87.

Lazzeroni P, Moretti F, Stirano F (2020). Economic potential of PV for Italian residential end-users. *Energy*, 200: 117508.

Lee DH (2016). Cost-benefit analysis, LCOE and evaluation of financial feasibility of full commercialization of biohydrogen. *International Journal of Hydrogen Energy*, 41: 4347–4357.

Li D, Liu G, Liao S (2015). Solar potential in urban residential buildings. *Solar Energy*, 111: 225–235.

Li C, Zhou D, Zheng Y (2018). Techno-economic comparative study of grid-connected PV power systems in five climate zones, China. *Energy*, 165: 1352–1369.

Liu P, Tan Z (2016). How to develop distributed generation in China: In the context of the reformation of electric power system. *Renewable and Sustainable Energy Reviews*, 66: 10–26.

Martinopoulos G (2020). Are rooftop photovoltaic systems a sustainable solution for Europe? A life cycle impact assessment and cost analysis. *Applied Energy*, 257: 114035.

Mohajeri N, Upadhyay G, Gudmundsson A, et al. (2016). Effects of urban compactness on solar energy potential. *Renewable Energy*, 93: 469–482.

MOHURD (1993). GB 50178-93: Standard of Climatic Regionalization for Architecture. Ministry of Housing and Urban-Rural Development of China. Beijing: China Architecture & Building Press. (in Chinese)

MOHURD (2012). GB 50797-2012: Code for Design of Photovoltaic Power Plants. Ministry of Housing and Urban-Rural Development of China. Beijing: China Architecture & Building Press. (in Chinese)

MOHURD (2019). GB 50352-2019: Uniform Standard for Design of Civil Buildings. Ministry of Housing and Urban-Rural Development of China. Beijing: China Architecture & Building Press. (in Chinese)

Obi M, Jensen SM, Ferris JB, et al. (2017). Calculation of levelized costs of electricity for various electrical energy storage systems. *Renewable and Sustainable Energy Reviews*, 67: 908–920.

Perez R, Hoff T, Herig C, et al. (2003). Maximizing PV peak shaving with solar load control: validation of a web-based economic evaluation tool. *Solar Energy*, 74: 409–415.

Ramírez-Sagner G, Mata-Torres C, Pino A, et al. (2017). Economic feasibility of residential and commercial PV technology: The Chilean case. *Renewable Energy*, 111: 332–343.

Reichelstein S, Yorston M (2013). The prospects for cost competitive solar PV power. *Energy Policy*, 55: 117–127.

Ren L, Zhao X, Yu X, et al. (2018a). Cost-benefit evolution for concentrated solar power in China. *Journal of Cleaner Production*, 190: 471–482.

Ren L, Zhao X, Zhang Y, et al. (2018b). The economic performance of concentrated solar power industry in China. *Journal of Cleaner Production*, 205: 799–813.

Spertino F, Di Leo P, Cocina V (2013). Economic analysis of investment in the rooftop photovoltaic systems: A long-term research in the two main markets. *Renewable and Sustainable Energy Reviews*, 28: 531–540.

Staudacher T, Eller, S (2012). SIMULATION-Dezentrale Stromversorgung eines Einfamilienhauses. *BWK-Das Energie Fachmagazin*, 64(6): 38. (in German)

Sun J, Liu Q, Duan Y (2018). Effects of evaporator pinch point temperature difference on thermo-economic performance of geothermal organic Rankine cycle systems. *Geothermics*, 75: 249–258.

Thiem S, Danov V, Metzger M, et al. (2017). Project-level multi-modal energy system design—Novel approach for considering detailed component models and example case study for airports. *Energy*, 133: 691–709.

Viana MS, Manassero G, Udaeta MEM (2018). Analysis of demand response and photovoltaic distributed generation as resources for power utility planning. *Applied Energy*, 217: 456–466.

Wang LZ, Tan HW, Ji L, Wang D (2017). A method for evaluating photovoltaic potential in China based on GIS platform. *IOP Conference Series*: *Earth and Environmental Science*, 93: 012056.

Xu S, Li Z, Zhang C, et al. (2021). A method of calculating urban-scale solar potential by evaluating and quantifying the relationship between urban block typology and occlusion coefficient: A case study of Wuhan in Central China. *Sustainable Cities and Society*, 64: 102451.

Yuan J, Sun S, Zhang W, et al. (2014). The economy of distributed PV in China. *Energy*, 78: 939–949.

Zhang F, Deng H, Margolis R, et al. (2015). Analysis of distributed-generation photovoltaic deployment, installation time and cost, market barriers, and policies in China. *Energy Policy*, 81: 43–55.

Zhao X, Zeng Y, Zhao D (2015). Distributed solar photovoltaics in China: Policies and economic performance. *Energy*, 88: 572–583.

Zhao X, Xie Y (2019). The economic performance of industrial and commercial rooftop photovoltaic in China. *Energy*, 187: 115961.